

- al., *Nature* **371**, 252 (1994); M. K. Webster and D. J. Donoghue, *EMBO J.* **15**, 520 (1996).
7. M. C. Naski et al., *Nature Genet.* **13**, 233 (1996).
 8. P. L. Tavormina et al., *ibid.* **9**, 321 (1995); M. K. Webster et al., *Mol. Cell. Biol.* **16**, 4081 (1996).
 9. M. Klagsbrun and E. R. Edelman, *Arteriosclerosis* **9**, 269 (1989); H. Brem and M. Klagsbrun, in *Oncogenes and Tumor Suppressor Genes in Human Malignancies*, C. C. Benz and E. T. Liu, Eds. (Kluwer Academic, Boston, 1993), p. 211; M. Klagsbrun and P. A. D'Amore, *Ann. Rev. Physiol.* **53**, 217 (1991).
 10. J. Adnane et al., *Oncogene* **6**, 659 (1991); F. Penault-Llorca et al., *Int. J. Cancer* **61**, 170 (1995); J. Jacquemier et al., *ibid.* **59**, 373 (1994); S. W. McLeskey, I. Y. Ding, M. E. Lippman, F. G. Kern, *Cancer Res.* **54**, 523 (1994); Y. A. Luqmani et al., *Int. J. Cancer* **64**, 274 (1995); S. Jaakkola et al., *ibid.* **54**, 374 (1993).
 11. H. Y. Leung, W. J. Gullick, N. R. Lemoine, *Int. J. Cancer* **59**, 667 (1994).
 12. F. Yamaguchi, H. Saya, J. M. Bruner, R. S. Morrison, *Proc. Natl. Acad. Sci. U.S.A.* **91**, 484 (1994); R. S. Morrison et al., *J. Neurooncol.* **18**, 207 (1994).
 13. Y. Myoken et al., *Int. J. Cancer* **65**, 650 (1996).
 14. J. J. Li et al., *Cancer* **72**, 2253 (1993).
 15. C. Theillet et al., *Genes Chromosomes Cancer* **7**, 219 (1993).
 16. M. T. Story, *World J. Urol.* **13**, 297 (1995); J. L. Ware, *Cancer Metastasis Rev.* **12**, 287 (1993).
 17. Preparation of 3-[4-(1-formylpiperazin-4-yl)benzylidene]-2-indolinone (SU4984) was as follows: A reaction mixture of 133.15 mg (1.0 mmol) of oxindole, 228.3 mg (1.2 mmol) of 4-(1-formylpiperazin-4-yl)benzaldehyde, and three drops of piperidine in 2 ml of ethanol was stirred at 90°C for 5 hours. After cooling, the precipitate was filtered, washed with cold ethanol, and dried to yield 199.5 mg (65%) of SU4984 as a yellow solid. Nuclear magnetic resonance (NMR) spectroscopy showed that SU4984 exists predominantly in the *trans* configuration (C-2, C-1'), although in the crystal structure, SU4984 is observed in the *cis* configuration. Preparation of 3-[(3-(2-carboxyethyl)-4-methylpyrrol-2-yl)methylene]-2-indolinone (SU5402) was as follows: A reaction mixture of 134.0 mg (1.0 mmol) of oxindole, 217.43 mg (1.2 mmol) of 3-(2-carboxyethyl)-4-methylpyrrol-2-carboxaldehyde, and three drops of piperidine in 3 ml of ethanol was stirred at 90°C for 3 hours. After cooling, the precipitate was filtered, washed with cold ethanol, and dried to yield 172.4 mg (58%) of SU5402 as a yellow solid. NMR spectroscopy showed that SU5402 exists predominantly in the *cis* configuration.
 18. The compounds were dissolved in dimethylsulfoxide (DMSO) as 100 mM stock solutions and stored at 4°C. The compounds were then diluted in DMSO to a concentration 20× the final concentration used in the *in vitro* kinase reactions. FGFR1K (9 μl) [2.2 mg/ml in 10 mM tris (pH 8) and 10 mM NaCl] was mixed with 1 μl of various concentrations of 20× SU4984 or 20× SU5402, or with 1 μl of DMSO (control). The reaction was started by adding 6 μl of the enzyme-compound mixture to 6 μl of 2× kinase buffer [2 mM ATP/[γ-³²P]ATP (10 μCi/μl), 4 mM MgCl₂ in 10 mM tris (pH 8), and 10 mM NaCl] at room temperature. At various time points, 2 μl of the reaction mixture was removed and added to 4 μl of 20 mM EDTA to stop the reaction. The reaction products were analyzed by SDS-PAGE (12% gel) and autoradiography. The radioactive bands were excised from the gel, and ³²P incorporation was quantitated by Cerenkov counting with a β counter.
 19. NIH 3T3 cells expressing endogenous FGF receptors were used. Cell culture, cell lysis, immunoprecipitation, and immunoblotting were carried out according to standard procedures. Anti-FGFR1 was described previously [M. Mohammadi et al., *Mol. Cell. Biol.* **16**, 977 (1996)].
 20. [³H]Thymidine incorporation was done as described by Mohammadi et al. (19).
 21. NIH 3T3 cells expressing endogenous PDGF receptors were used. Also used were HER14 cells (33) and NIH1R cells [S. J. Isakoff et al., *J. Biol. Chem.* **271**, 3959 (1996)]. The EGF receptor was immunoprecipitated with monoclonal antibody 108 (33), insulin receptor with monoclonal antibodies (BBE) [N. P. Moller et al., *J. Biol. Chem.* **270**, 23126 (1995)], and PDGF receptor with polyclonal antibodies (PR4) [S. Mori et al., *EMBO J.* **12**, 2257 (1993)].
 22. M. Mohammadi, J. Schlessinger, S. R. Hubbard, *Cell* **86**, 577 (1996).
 23. S. S. Taylor and E. Radzio-Andzelm, *Structure* **2**, 345 (1994).
 24. K. A. Thomas, G. M. Smith, T. B. Thomas, R. J. Feldman, *Proc. Natl. Acad. Sci. U.S.A.* **79**, 4843 (1982).
 25. G. McMahon, unpublished results.
 26. S. R. Hubbard, in preparation.
 27. _____, L. Wei, L. Ellis, W. A. Hendrickson, *Nature* **372**, 746 (1994).
 28. R. M. Lyall et al., *J. Biol. Chem.* **264**, 14503 (1989); B. Margolis et al., *Cell* **57**, 1101 (1989).
 29. W. F. De Azevedo et al., *Proc. Natl. Acad. Sci. U.S.A.* **93**, 2735 (1996); U. Schulze-Gahmen et al., *Proteins Struct. Funct. Genet.* **22**, 378 (1995).
 30. R.-M. Xu, G. Carmel, J. Kuret, X. Cheng, *Proc. Natl. Acad. Sci. U.S.A.* **93**, 6308 (1996).
 31. R. A. Engh, A. Girod, V. Kinzel, R. Huber, D. Bossemeyer, *J. Biol. Chem.* **271**, 26157 (1996).
 32. M. G. Malkin, W. P. Mason, F. S. Lieberman, L. K. Shawver, A. L. Hannah, in *Proceedings of the 32nd Annual Meeting of the American Society of Clinical Oncology*, Philadelphia, PA, 18 to 21 May 1996 (American Society of Clinical Oncology, Philadelphia, PA, 1996), vol. 15, p. 1573.
 33. A. M. Honegger et al., *Cell* **51**, 199 (1987).
 34. S. V. Evans, *J. Mol. Graphics* **11**, 134 (1993).
 35. A. Nicholls, K. A. Sharp, B. Honig, *Proteins* **11**, 281 (1991).
 36. Z. Otwinowski, in *Data Collection and Processing*, L. Sawyer, N. Isaacs, S. Bailey, Eds. (SERC Daresbury Laboratory, Warrington, UK, 1993), p. 56.
 37. A. T. Brünger, *X-PLOR Version 3.1: A System for X-ray and NMR* (Yale Univ. Press, New Haven, CT, 1992).
 38. T. A. Jones, *Methods Enzymol.* **115**, 157 (1985).
 39. Equipment in the structural biology program at the Skirball Institute is partially supported by a grant from the Kresge Foundation. Coordinates have been deposited in the Brookhaven Protein Data Bank, entries 1FGI and 1AGW.

31 January 1997; accepted 11 March 1997

Kinetics of Response in Lymphoid Tissues to Antiretroviral Therapy of HIV-1 Infection

Winston Cavert, Daan W. Notermans, Katherine Staskus, Stephen W. Wietgreffe, Mary Zupancic, Kristin Gebhard, Keith Henry, Zhi-Qiang Zhang, Roger Mills, Hugh McDade, Jaap Goudsmit, Sven A. Danner, Ashley T. Haase*

In lymphoid tissue, where human immunodeficiency virus-type 1 (HIV-1) is produced and stored, three-drug treatment with viral protease and reverse transcriptase inhibitors markedly reduced viral burden. This was shown by *in situ* hybridization and computerized quantitative analysis of serial tonsil biopsies from previously untreated adults. The frequency of productive mononuclear cells (MNCs) initially diminished with a half-life of about 1 day. Surprisingly, the amount of HIV-1 RNA in virus trapped on follicular dendritic cells (FDCs) decreased almost as quickly. After 24 weeks, MNCs with very few copies of HIV-1 RNA per cell were still detectable, as was proviral DNA; however, the amount of FDC-associated virus decreased by ≥3.4 log units. Thus, 6 months of potent therapy controlled active replication and cleared >99.9 percent of virus from the secondary lymphoid tissue reservoir.

In HIV-1 infection, the measurement of viral load in plasma is a useful guide to prognosis and to the efficacy of antiretroviral therapy (1). Ultimately, however, the impact of treatment can only be assessed

completely in the lymphoid tissue (LT) reservoirs, where most of the virus is produced by CD4⁺ T lymphocytes, macrophages, and other lymphoid MNCs and is stored in immune complexes on the surfaces of FDCs. In the asymptomatic stage of infection, the pool of virus on FDCs is at least an order of magnitude greater than that in MNCs (2). In turn, both LT viral compartments exceed by orders of magnitude the quantity of free and cell-associated virus circulating in the bloodstream. In reports published to date, the LT viral pools are little affected by monotherapy with nucleoside analog drugs that inhibit reverse transcriptase (RTIs) (2, 3) and are only moderately reduced by therapy with two or three RTIs (4, 5).

We investigated the effect of treatment with a more potent antiretroviral drug combination on viral burden in serial tonsil

W. Cavert, K. Staskus, S. W. Wietgreffe, M. Zupancic, K. Gebhard, Z.-Q. Zhang, A. T. Haase, Department of Microbiology, University of Minnesota Medical School, Minneapolis, MN 55455, USA.

D. W. Notermans, J. Goudsmit, S. A. Danner, Division of Infectious Diseases, Tropical Medicine, and AIDS and National AIDS Therapy Center, Academic Medical Center, University of Amsterdam, Post Office Box 22700, 1100 DE Amsterdam, Netherlands.

K. Henry, HIV Program, St. Paul-Ramsey Medical Center, St. Paul, MN 55101, USA, and Department of Medicine, University of Minnesota Medical School, Minneapolis, MN 55455, USA.

R. Mills, Abbott Laboratories, Abbott Park, IL 60064, USA.

H. McDade, Glaxo Wellcome Research and Development, Greenford-Middlesex UB6 0HE, UK.

*To whom correspondence should be addressed.

biopsies (6), which have been shown to be representative of the secondary LT in HIV-1 infection (2). We used a technique that combined in situ hybridization with computer-assisted quantitative image analysis to measure and differentiate HIV-1 RNA in virus-producing MNCs and in virion-antibody immune complexes deposited on FDCs (2). Biopsies were obtained from participants with visible tonsils in an LT substudy of a clinical treatment trial combining a potent HIV-1 protease inhibitor, ritonavir, and two RTIs, zidovudine and lamivudine. All participants in the parent study received ritonavir throughout, whereas both RTIs were initiated either upon enrollment (immediate group) or 3 weeks later (delayed group) to test the hypothesis that initial reductions in viral replication would forestall the development of drug resistance against RTIs. Thirty-four previously untreated HIV-1-seropositive adults with absolute CD4⁺ cell counts of ≥50 cells per cubic millimeter and plasma HIV-1 RNA levels of ≥30,000 copies per milliliter were randomized in this open label trial (7). After 6 months of treatment, plasma HIV-1 RNA levels decreased at least 2.9 log units in both groups from a pretreatment median load of 5.3 log units (8).

Participants underwent tonsil biopsy 2 weeks before and 2 days, 22 days, and 24 weeks after treatment commenced. Because we could only obtain a few tonsil biopsies from any one individual, we chose time points to detect anticipated early rapid changes in the MNC compartment and more gradual changes in the FDC-associated pool. We based our selection of time points on published dynamic models of HIV-1 infection that predict a rapid turnover of productively infected MNCs (9, 10). We chose the later time points on the basis of previous work describing the protracted retention of conventional virus-containing antigen-antibody complexes by FDCs (11), the apparent stability of the FDC-HIV association (12), and the enormity of the FDC-associated HIV-1 reservoir (2). From these previous observations, we expected a much slower turnover of FDC-complexed virus.

Each tonsil biopsy was cut in half. One portion was fixed and embedded in paraffin; the other portion was flash-frozen for later extraction and assay of viral nucleic acids. Paraffin blocks were then sectioned and hybridized in situ to a ³⁵S-labeled RNA probe complementary to >90% of the sequences in HIV-1 RNA. After autoradiography, the hybridization signal overlying FDCs or MNCs was quantitated by computer-assisted image analysis (2).

We obtained sequential tissue samples

suitable for evaluation from 10 individuals (13). At baseline, this cohort had a mean of 1.5×10^8 copies of viral RNA per gram on FDCs (Table 1) (14), equal to the mean concentration previously measured at an earlier stage of infection (2). By contrast, the mean frequency of MNCs with >20 copies of HIV-1 RNA per cell was 3.1×10^5 cells per gram (Table 1). In

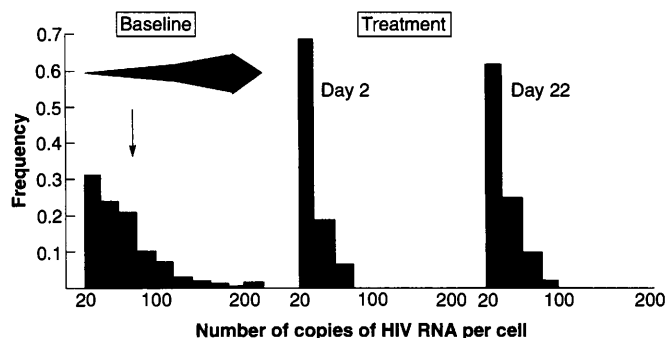
these individuals with more advanced HIV-1 infection, the MNC pool thus proved to be larger than in earlier HIV disease stages (2). The result, however, is consistent with the higher mean baseline plasma HIV-1 RNA levels that imply greater rates of virus production.

After 2 days of treatment, we observed a rapid drop from baseline in the frequency of

Table 1. Effect of combination antiretroviral therapy on HIV stored on FDCs and on productively infected MNCs (those with >20 copies of HIV RNA per cell) in LT. Tonsil biopsies were obtained from 10 HIV-infected adults within 14 days before initiating treatment with ritonavir, zidovudine, and lamivudine, and at the designated times thereafter. One-half of the biopsy was fixed in Streck's tissue fixative for 24 hours, stored for 3 to 10 days in 80% ethanol, and then embedded in paraffin. Sections (8 μm) were cut, pretreated, and hybridized in situ to a ³⁵S-labeled HIV-specific antisense probe, as described (16). After hybridization, the sections were washed, coated with nuclear track emulsion, and, after 1 day of autoradiographic exposure, developed and stained. The number of copies of HIV RNA per gram on FDCs in baseline, day 2, day 22, and week 24 biopsies was calculated from the number of silver grains determined by quantitative image analysis contained within the cumulative areas of 10 or more sections, as described (2). Productively infected MNCs are easily identified in tissue sections with 1-day exposures. Asterisks denote week 24 biopsies containing detectable MNCs with <10 copies of HIV RNA per cell after 10-day exposures. Time points at which the available tonsil biopsy was inadequate for analysis (usually because the tissue was almost entirely epithelial) are indicated by -. See (18) for a description of how the limits of detection were determined.

Patient	Biopsy	Number of copies of HIV RNA per gram on FDCs	Frequency (MNCs per gram) with >20 copies of HIV RNA per cell
1	Baseline	3.0×10^8	4.6×10^5
	Day 2	5.9×10^7	2.6×10^5
	Day 22	6.0×10^7	9.0×10^4
	Week 24	3.9×10^5	$<1.2 \times 10^3$
2	Baseline	1.6×10^8	9.7×10^5
	Day 2	7.1×10^7	4.5×10^4
	Day 22	-	-
	Week 24	$\leq 10^4$	$<8.6 \times 10^2$ *
3	Baseline	3.5×10^8	2.5×10^5
	Day 2	1.9×10^8	1.2×10^5
	Day 22	1.7×10^8	1.2×10^5
	Week 24	2.5×10^5	$<7.1 \times 10^2$ *
4	Baseline	2×10^7	4.0×10^4
	Day 2	1.9×10^7	2.5×10^4
	Day 22	2×10^6	1.3×10^3
	Week 24	1.4×10^4	$<7.7 \times 10^2$ *
5	Baseline	2.0×10^8	5.0×10^5
	Day 2	4.4×10^7	2.6×10^3
	Day 22	1.8×10^7	1.0×10^3
	Week 24	$\leq 10^4$	$<3.0 \times 10^2$
6	Baseline	-	-
	Day 2	2.8×10^8	7.0×10^4
	Day 22	4.4×10^7	7.5×10^3
	Week 24	1.7×10^4	$<9.4 \times 10^2$
7	Baseline	1.3×10^8	1.4×10^5
	Day 2	3.9×10^7	1.5×10^4
	Day 22	1.4×10^6	3.7×10^3
	Week 24	$\leq 10^4$	$<1.3 \times 10^3$ *
8	Baseline	6.2×10^7	2.0×10^5
	Day 2	1.8×10^7	2.0×10^4
	Day 22	-	-
	Week 24	2.6×10^5	$<6.9 \times 10^2$ *
9	Baseline	2.5×10^7	6.5×10^4
	Day 2	1.1×10^7	1.5×10^4
	Day 22	3.0×10^6	4.1×10^3
	Week 24	$\leq 10^4$	$<1.0 \times 10^3$
10	Baseline	1.3×10^8	1.5×10^5
	Day 2	1.6×10^8	1.2×10^5
	Day 22	1.7×10^7	4.0×10^3
	Week 24	2.7×10^5	$<2.4 \times 10^3$
Baseline mean		1.5×10^8	3.1×10^5

Fig. 1. Representative frequency distribution of viral RNA copies per MNC in LT before (baseline) and 2 and 22 days after treatment. Two days after initiating treatment, most of the cells with >75 copies of HIV RNA per MNC at baseline (vertical arrow) have been eliminated from the distribution. These cells are infected cells at later stages of the viral life cycle (represented by a large, spreading horizontal arrow). The frequency distribution of the number of copies of viral RNA per cell was determined by in situ hybridization and quantitative image analysis for ≥ 100 cells at each time point for each biopsy.



MNCs with the highest intracellular concentration of viral RNA, those with >75 copies of HIV-1 RNA per cell (Fig. 1). These MNCs (the right tail of the frequency distribution in Fig. 1A) disappeared quickly with treatment, which affirms our previous proposal that this population consists of cells in the late stages of the viral life cycle in infections that were initiated asynchronously in vivo (2). This subpopulation of infected cells with the highest intracellular concentration of HIV-1 turns over rapidly and contributes most of the daily viral production.

From the data summarized in Table 1 and displayed in Fig. 2A, we estimate a steady-state half-life of $t_{1/2} = 0.9$ days for the population of MNCs in the later stages of a productive infection. This half-life corresponds to a turnover rate of 1.2×10^5 cells $g^{-1} day^{-1}$, or $\sim 8 \times 10^7$ cells in a 70-kg person (assuming LT is 1% of total body weight) (14). This directly measured rate of infected MNC turnover is about four times the rate we estimated previously for individuals in an earlier stage of HIV-1 infection (2). However, the faster rate of turnover implies a greater production of virus and is consistent with the higher plasma

HIV-1 RNA levels (8).

In vitro studies of FDC interactions with HIV-1 have shown that virus remains tightly bound to the FDCs for at least several days (12). For this reason, we had not anticipated the surprisingly rapid initial rate of elimination of virus from FDCs that we observed. The loss from FDCs closely followed the rapid decline in the number of productively infected lymphoid MNCs (Fig. 2) and in the amount of plasma HIV-1 RNA (8). From the half-life of FDC HIV-1 RNA ($t_{1/2} = 1.7$ days), we calculate an initial clearance rate of 4.3×10^7 copies $g^{-1} day^{-1}$ of viral RNA, or $\sim 2.1 \times 10^7$ virions $g^{-1} day^{-1}$ for the FDC pool. We interpret this ability of the FDC pool as evidence of a pretreatment state in which the binding and dissociation of virion-antibody complexes from FDCs is in equilibrium with the production and clearance of virus from the peripheral circulation. When potent therapy reduces the amount of newly produced virus available to bind to FDCs, clearance and dissociation continue apace, and consequently the FDC pool quickly shrinks.

Because the source of virus and the largest pool of virus are at steady state before treatment, we can directly estimate pre-

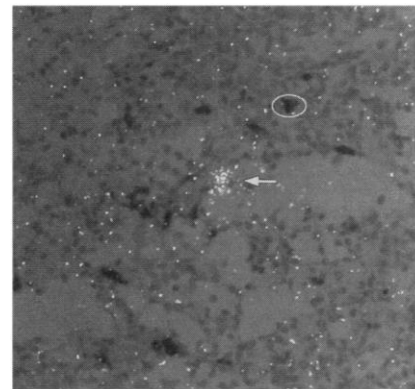
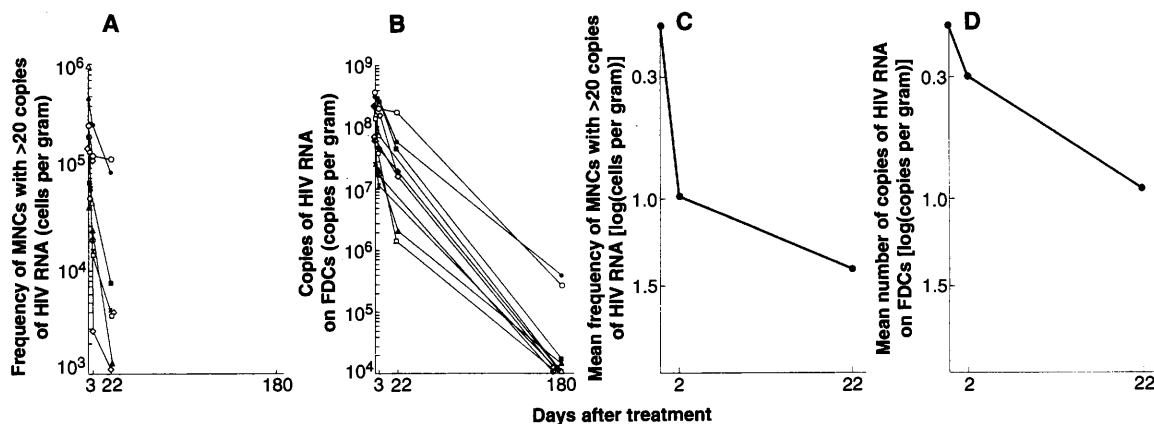


Fig. 3. Macrophages after treatment. Double-label in situ hybridization (16, 17) was used to identify macrophages and HIV RNA in MNCs. In the developed autoradiographs of tonsil tissue obtained 22 days after treatment, most cells with the greatest concentration of HIV RNA are not macrophages. In this image, trans- and epipolarized light make silver grains appear white, indicating HIV RNA in a cell (arrow). The HIV RNA hybridization signal does not colocalize with the dark macrophages (circled area) that have been stained immunohistochemically with CD68 mAb (original magnification, $\times 400$).

treatment virus production in vivo from the initial decrease in productive cells and from the virus lost from the FDC pool (14). From the initial loss of $\sim 1.2 \times 10^5$ productively infected cells $g^{-1} day^{-1}$ of LT and the decrease of 2.1×10^7 virions $g^{-1} day^{-1}$ in LT, we estimate that each cell produces ~ 175 HIV-1 virions. This dynamic measurement of HIV-1 production is in good agreement with our previous indirectly derived estimates (2) and is also consonant with published estimates derived from plasma virus clearance of $\sim 10^{10}$ virions per day (10, 15).

By day 2, more than 75% of the infected MNCs contained only 20 to 60 copies of HIV-1 RNA each, a considerable reduction in the productive burst size. Between day 2 and day 22 of treatment (Fig. 2, C and D),

Fig. 2. Effect of treatment on the frequency of productively infected MNCs and on viral burden associated with FDCs in LT. The frequency of productively infected MNCs (A) and the number of copies of HIV-1 RNA on FDCs (B) were determined as described in Fig. 1 and Table 1 and were plotted against days of treatment for all 10 patients (represented by the various symbols). Over the course of the first 22 days of treatment, changes in the two cellular compartments parallel each other with initially rapid and then slower rates of decrease. (C and D) Mean decreases for the LT study group as a whole (in log units).



the MNC and FDC pools continued to decay in parallel with one another, but with slower kinetics ($t_{1/2} \approx 15$ and 14 days, respectively). In addition, we found many MNCs with >20 but <75 copies of HIV-1 RNA in the third week of treatment (Fig. 1). It is possible that these cells with lower concentrations of intracellular RNA are cells that are blocked at an early phase of the viral life cycle and did not progress to later stages after 3 weeks of treatment. However, it is more likely that these cells represent a longer lived subpopulation of cells infected before initiation of treatment. The continued production of smaller amounts of virus by this subpopulation of MNCs would partially compensate for the ongoing clearance from the FDC-associated viral pool and thereby for the parallel and slower rate of decay in the FDC virus pool between days 2 and 22.

Because infected macrophages might fulfill the criteria of longer lived cells with lower levels of viral RNA, we examined day 22 tissue sections for evidence of HIV-1 RNA in macrophages by a double-label technique (16). Sections that had been hybridized in situ to detect HIV-1 RNA were stained immunohistochemically with CD68 monoclonal antibody (mAb) to unambiguously identify macrophages (17). In these experiments, a few macrophages containing HIV-1 RNA were identified, but at day 22 of treatment, the vast majority of the cells in which viral RNA could be detected did not stain with CD68 mAb (Fig. 3).

Between 3 and 24 weeks of treatment, the number of MNCs with >20 copies of HIV-1 RNA per cell fell to undetectable amounts in all 10 LT substudy participants (mean decrease in cells per gram, >2.3 log units), as did the amount of FDC-associated HIV-1 RNA in most individuals (mean decrease in HIV-1 RNA copies per gram, ≥ 3.4 log units). To extend the analysis to residual pools of virus and infected cells, we

lengthened the autoradiographic exposure time of 1 day (appropriate for quantitating large amounts of HIV-1 RNA) to 10 days. We thus increased the limits of sensitivity to about one HIV-1 RNA copy per cell (18). With this more sensitive assay, we found considerable heterogeneity in the subjects' treatment response at 6 months. In 6 of 10 individuals, there was a mean residue of 2×10^5 copies of HIV-1 RNA per gram on FDCs (Fig. 4, A and B), equivalent to $\sim 10^8$ virions in a 70-kg individual. With these longer exposures, in five individuals we also observed 10^3 to 10^4 MNCs per gram with fewer than 10 copies of HIV-1 RNA per cell (Fig. 4C). At week 24 of treatment in one individual (patient 5, Table 1), we could not detect any trace of residual HIV-1 RNA in either cellular compartment, down to a sensitivity of <300 cells per gram for cells with at least one copy of viral RNA per cell.

In 6 of the 10 subjects (patients 1 to 6, Table 1), frozen tonsil tissue specimens were available for study. Nucleic acid extracted from the frozen portion of the week 24 biopsy of patient 5 also lacked detectable HIV-1 RNA, as assessed by a nested reverse transcription polymerase chain reaction (RT-PCR). However, in all six patients for whom frozen biopsy specimens were available, HIV-1 DNA was detectable by nested PCR amplification of proviral DNA extracted from the week 24 frozen biopsy (19).

After 6 months of triple therapy, LT still harbors infected cells, and in some of these cells there is evidence of low levels of viral gene expression. The life-span and function in HIV-1 disease of MNCs in which we can still detect small amounts of viral RNA requires further investigation, but as long as they and latently infected cells (20) live, there will be reason to continue treatment. Despite the persistent infection, the number of copies of HIV-1 RNA per gram cleared from LT was ≥ 3.4 log units over

just 6 months of therapy. If continued at the same rate seen between 3 weeks and 6 months, this extrapolates to elimination of viral RNA within an average of 30 months of triple antiretroviral therapy. Further studies will be necessary to ascertain whether it is possible to completely purge HIV-1 infection from LT, or whether lifelong maintenance therapy will be required after initial "induction" treatment. Nevertheless, we have shown that within 6 months, triple drug therapy eliminates more than 99% of the lymphoid cells actively producing the virus that is responsible for immune depletion (21).

REFERENCES AND NOTES

1. J. W. Mellors *et al.*, *Science* **272**, 1167 (1996); D. A. Katzenstein *et al.*, *N. Engl. J. Med.* **335**, 1091 (1996); W. A. O'Brien *et al.*, *ibid.* **334**, 426 (1996).
2. A. T. Haase *et al.*, *Science* **274**, 985 (1996).
3. O. J. Cohen *et al.*, *J. Infect. Dis.* **173**, 849 (1996).
4. O. J. Cohen *et al.*, *Proc. Natl. Acad. Sci. U.S.A.* **92**, 6017 (1995).
5. A. Lefeuvre *et al.*, *J. Infect. Dis.* **174**, 404 (1996).
6. R. A. Faust *et al.*, *Otolaryngol. Head Neck Surg.* **114**, 593 (1996).
7. Protocol NUCB 2019. Participants underwent serial venipuncture for T cell subsets, plasma HIV RNA, and genotypic virology.
8. D. W. Notermans *et al.*, in preparation.
9. X. Wei *et al.*, *Nature* **373**, 117 (1995); D. D. Ho *et al.*, *ibid.*, p. 123.
10. A. S. Perelson *et al.*, *Science* **271**, 1582 (1996).
11. T. E. Mandel *et al.*, *Immunol. Rev.* **53**, 29 (1980).
12. S. L. Heath *et al.*, *Nature* **377**, 740 (1995).
13. Seventeen individuals underwent at least one tonsil biopsy. Four subjects withdrew from the LT substudy because early biopsies provided insufficient LT for analysis, and three withdrew for clinical reasons. Of the 10 remaining, all had evaluable tissue at three or all four of the time points, and all had final biopsies at 6 months. Their median baseline peripheral absolute CD4⁺ cell count was 194 cells per cubic millimeter.
14. Viral load in FDC and MNC pools and frequency of infected cells per gram of LT were determined at baseline (2) and at 24 weeks (18) as described. Half-lives for the FDC-associated viral load and the frequency of MNCs with >20 copies of viral RNA per cell were estimated by solving the equation $t_{1/2} = n / [\log(\text{mean } v_0 / \text{mean } v_t) / \log 2]$, where n = number of days and v = viral load at each time point. The initial turnover rates were calculated from the $t_{1/2}$ values, the mean pool sizes shown in Table 1, and the number of days of treatment. Because the FDC pool stores most virus produced, the simplest explanation for the early rapid elimination of FDC-associated virus is that it is a result of treatment-induced reductions in MNC virus manufacture. Dividing the initial turnover per day in the FDC pool by the initial turnover per day of MNC thus gives an estimate of the number of copies of viral RNA per productively infected MNC.
15. J. M. Coffin, *Science* **267**, 483 (1995).
16. M. Brahic and A. T. Haase, *Curr. Top. Microbiol. Immunol.* **143**, 9 (1989).
17. To unambiguously identify the cell type in which HIV RNA is detectable, we combined in situ hybridization and immunohistochemical staining with mAb to CD68, a macrophage-specific marker. Tissue sections were deparaffinized with xylene, cleared with ethanol, and hydrated in diethyl pyrocarbonate (DEPC) water. CD68 antigen reactivity with the mAb was enhanced by heating the slides for 10 min at 80% power of a 1000-W microwave oven in 10 mM citrate buffer (pH 6.0). After cooling for 30 min, the sections were acetylated, prehybridized, and then hybridized with antisense ³⁵S-labeled HIV RNA

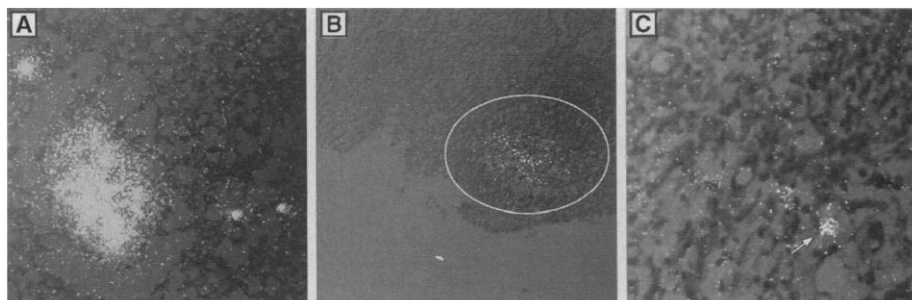


Fig. 4. Viral burden in LT after 24 weeks of treatment. The sensitivity of detection of infected cells and residual HIV RNA in FDCs was increased by an order of magnitude by lengthening the autoradiographic exposure time. Before treatment (A), a large and diffuse hybridization signal (silver grains) overlies FDCs in a GC. Dense collections of silver grains overlie three infected MNCs. At 24 weeks, signals are greatly reduced but still detectable in some cells and GCs (B and C). The circled area in (B) defines a GC with 150 copies of HIV RNA on FDCs. The arrow in (C) denotes a MNC with <10 copies of HIV RNA. Original magnifications, $\times 160$ (A and B) and $\times 400$ (C).

probe. After post-hybridization washes, nonspecific binding of antibodies was blocked by immersing the sections in 5% nonfat milk in phosphate-buffered saline (PBS) for 30 min. Sections were then treated with a 1:300 dilution of CD68 mAb (Dako, Carpinteria, CA) at 4°C overnight. After washing, slides were developed with a peroxidase-conjugated secondary antibody and diaminobenzidine substrate according to the manufacturer's protocol (ABC Elite kit; Vector Labs, Burlingame, CA). The sections were then washed in PBS and 0.1 × PBS, dehydrated in ethanol containing 0.3 M ammonium acetate, and coated with nuclear track emulsion. After development, the slides were briefly counterstained in hematoxylin.

18. Longer autoradiographic exposures of 7 to 10 days increase the sensitivity of in situ hybridization. To determine the limits of detection of HIV RNA, we first measured the background signal over MNCs and FDCs from the binding of antisense HIV RNA probe to LT sections of HIV-seronegative individuals and from the nonspecific binding of the sense HIV RNA probe to LT sections of HIV-seropositive individuals. Dividing the number of silver grains determined by quantitative image analysis in randomly selected areas by the number of cells in those areas provided a maximum estimate of background. Backgrounds by both approaches were one or two silver grains per MNC for 10-day exposures. An MNC with one HIV RNA copy will show 24 grains over background with such long exposures and will be easily identified. The lower limit of detection for MNCs is therefore about one copy of HIV RNA per cell. For the FDCs, we measured the area of germinal centers (GCs) and determined their average backgrounds to be 2.3 grains per 10⁻³ mm². The Poisson probability that x number of grains differs from a background average of m grains is $1 - m^x \exp(-m) m(x!)^{-1}$ (22). For a probability $P > 0.99$ that there is a significant increase over background in a GC, the signal over FDCs would have to be more than seven grains per 10⁻³ mm². For example, the GC shown in Fig. 4B had 450 grains in an area of 0.05 mm², or 9 grains per 10⁻³ mm², and thus fulfills this condition; from the number of silver grains over background, we calculate that there are 146 copies of HIV-1 RNA in this GC. The limits of detection of viral RNA for infected cells expressed per gram of tissue depends on the number and area of the sections examined. For example, we usually randomly sampled and exhaustively screened 40 8- μ m sections averaging ~5 mm² each, cumulatively equivalent to ~1.2 mg of tissue. If these sections contained no MNCs with HIV-1 RNA, this frequency would be <~625 cells per gram. For the FDCs, we determined with the long exposure an average detectable copy number of ~20 copies per GC and thus a lower detection threshold of ~10⁴ copies per gram of LT.

19. For DNA PCR analysis, nucleic acids from guanidine-HCl extracts of flash-frozen tonsil biopsies were precipitated out of 70% ethanol, pelleted, ethanol-washed, and resuspended in 10 mM tris-HCl (pH 8.0) containing 1 mM EDTA and 0.5% SDS. The suspensions were then treated with ribonuclease A (RNase A, 20 μ g/ml) for 1 hour at 37°C, incubated with proteinase K (100 μ g/ml) at 50°C for 3 hours, and finally extracted with phenol, phenol/chloroform, and chloroform before ethanol precipitation and wash. Control DNA, with and without HIV-1 proviral DNA, was similarly extracted from ACH-2 cells and H-9 cells, respectively. Nested PCR was performed with the use of two sets of primers designed to amplify a conserved region of HIV-1 gag. The primary amplification reactions contained 1 μ g of each DNA specimen, 1 × PCRII reaction buffer (Perkin-Elmer), 2.5 mM MgCl₂, 20 mM deoxynucleotide triphosphates, 1 μ M primers (30-nucleotide oligomers: 5'-GTCAGCCAAAT-TACCCCTATAGTGCAGAAC-3', 5'-ACATAGTCTCT-AAAGGGTTCCTTTGGTCCT-3'), and Amplitaq polymerase (0.08 U/ml, Perkin-Elmer) in a 100-ml volume. DNA was amplified 25 cycles at 94°C for 45 s, 60°C for 45 s, and 72°C for 3 min. The secondary (nested) reactions contained 2 μ l of the primary amplified reaction mixture with otherwise the same constituents, except for primers (20-nucleotide oligomers: 5'-TCACCTAGAACTTTAAATGC-3', 5'-AT-

TTAATCCAGGATTATCC-3'). This second amplification was 30 cycles with the same cycling parameters. RT-PCR reactions were performed on RNA containing fractions of the guanidine tissue homogenates and were processed and PCR-amplified in the same manner, except that deoxyribonuclease pretreatment was substituted for RNase A pretreatment and reverse transcription using rTth polymerase (Perkin-Elmer) was included before amplification. Southern (DNA) blots were hybridized to a cocktail containing three oligonucleotide probes labeled at the 3' termini with [³²P]deoxyadenosine triphosphate specific for sequences internal to the nesting primers (30-nucleotide oligomers: 5'-CATGGGTAAAAGTAG-TAGAAGAGAAGGCTT-3', 5'-GGGACATCAAGCAGCCATGCAAATGTTAAA-3', 5'-CCAAGGGGAAGT-GACATAGCAGGAAGTACT-3').

20. J. Embretson *et al.*, *Nature* **362**, 359 (1993).
21. This marked reduction in lymphoid viral load translates into a slow but commensurate repopulation of the LT with CD4⁺ T lymphocytes (Z.-Q. Zhang *et al.*, in preparation).
22. A. T. Haase, in *In Situ Hybridization: Applications to Neurobiology*, K. L. Valentino, J. H. Eberwine, J. D. Barchas, Eds. (Oxford Univ. Press, New York, 1987), pp. 197-219.
23. We thank P. Dailey for technical assistance; C. O'Neill, T. Leonard, and G. Sedgewick for assistance with preparation of the manuscript and figures; and J. Leonard and G. Goodwin for clinical support. Supported by NIH grants AI 25017 and AI 28246.

9 January 1997; accepted 6 March 1997

TECHNICAL COMMENTS

Interactions Between Epithelial Cells and Bacteria, Normal and Pathogenic

Lynn Bry *et al.* show that the monoassociation of germ-free (GF) mice with wild-type *Bacteroides thetaiotaomicron* induced expression of an α 1,2 fucosyltransferase messenger RNA and production of fucosylated glycoconjugates that were reactive with *Ulex europaeus* agglutinin I in the epithelial cells of the small intestine (1). A mutant mouse strain that lacks the ability to utilize L-fucose did not induce efficient epithelial fusion. We have also observed the induction of an α 1,2 fucosyltransferase that mediates the synthesis of the fucosyl asialoGM1 glycolipid of small intestinal epithelial cells during the first stage of microbial colonization (conventionalization) in GF mice (2). Recently, we found that this fucosylation was induced by an indigenous bacteria [segmented filamentous bacteria (SFB) (3), which was identified on the basis of its 16S ribosomal DNA sequence (4)] and that it resulted in expression of major histocompatibility complex class II (MHC II) molecules, expansion of intraepithelial lymphocytes (IEL), and increase in immunoglobulin A (IgA)-producing cells. Within a month after SFB colonization, the columnar cell-to-goblet cell ratio and the mitotic activity of cryptal cells were almost the same as those found in wild-type mice. We have also found that when the SFB colonization in the conventionalization process was selectively inhibited by the oral administration of a monoclonal antibody against SFB, MHC II expression, and the growth of $\alpha\beta$ -T cell receptor-bearing IELs and IgA-producing cells were repressed (5). Thus, SFB seem to be essential for altering or accelerating the development of the small intestine. These events should occur in the weaning stage in the case of conventional mice with a normal intestinal microflora.

Alteration of the developmental program

did not occur in the course of association of GF mice with indigenous microbes derived from rat or human feces (6). SFB derived from mice and rats did not cross-colonize in rats and mice, respectively (7). There appears to be a strict limit to the interaction between the host animal and the intestinal bacteria, in accord with the concept of "autochthonous bacteria" proposed by Dubos *et al.* more than 30 years ago (8). Does the association of GF mice with *B. thetaiotaomicron* induce class II expression, expansion of IEL and IgA-producing cells, and so on after the expression of an α 1,2 fucosyltransferase? What is the original host of this bacterium, mouse or human? A GDP-fucose:asialo GM1 α 1,2 fucosyltransferase was induced in GF mice on injury to the small intestine (9). In our study, α 1,2 fucosyltransferase induction was the first event. We have no evidence, however, to suggest that this fucosylation initiates the developmental program of the intestinal mucosa, including the components in the lamina propria.

Yoshinori Umesaki
Yasushi Okada
Akemi Imaoka
Hiromi Setoyama
Satoshi Matsumoto
Yakult Central Institute for
Microbiological Research,
Yaho 1796, Kunitachi,
Tokyo 186, Japan
E-mail: hfg00420@niftyserve.or.jp

REFERENCES AND NOTES

1. L. Bry, P. G. Falk, T. Midtvedt, J. I. Gordon, *Science* **273**, 1380 (1996).
2. Y. Umesaki, T. Sakata, T. Yajima, *Biochem. Biophys. Res. Commun.* **105**, 439 (1982).
3. Y. Umesaki, Y. Okada, S. Matsumoto, A. Imaoka, H. Setoyama, *Microbiol. Immunol.* **39**, 555 (1995).
4. J. Snel *et al.*, *Int. Syst. Bacteriol.* **45**, 780 (1995).